ЖЭТФ, 2005, том 128, вып. 2 (8), стр. 351–363

SHORT-RANGE FERROMAGNETISM AND TRANSPORT PROPERTIES OF AMORPHOUS $(Gd,Y)_xSi_{1-x}$ ALLOYS

S. Caprara

Dipartimento di Fisica, Università di Roma «La Sapienza», Istituto Nazionale per la Fisica della Materia-SMC and UdR di Roma 1 00185 Rome, Italy

V. V. Tugushev [*]***, N. K. Chumakov*** [**]

RRC Kurchatov Institute 123182, Moscow, Russia

Submitted 31 January 2005

We present a theoretical description and electrical conductivity measurements for amorphous $(Gd,Y)_xSi_{1-x}$ alloys with $0.1 < x < 0.2$. In our model, we take into account the strong topological disorder in the system, causing the appearance of regions with higher electron density (electron «drops») around nanoscale structural defects enriched with rare-earth ions («clusters»). We calculate the local density of electron states in the drops and in the matrix and establish the criterion for local instability towards ferromagnetism. In the framework of the «local phase transition» approach, we find that short-range ferromagnetic order is more favorable inside the drops than in the matrix and exists in a wide temperature range. We analyze recent measurements of the temperature and magnetic-field dependence of the electrical conductivity in these systems and show that the spin polarization of the electron states in the drops enhances the tendency towards the metal–insulator transition.

PACS: 72.15.-Gd, 75.25.+z, 75.47.De, 75.50.Kj, 75.50.Pp

1. INTRODUCTION

The anomalous transport and magnetic properties of amorphous (a-) RE_xSi_{1-x} alloys (with RE = Gd, Tb, Y and $0.1 < x < 0.2$) have been the object of a controversial debate in recent years. The standard approach to these systems, described as disordered magnetic semiconductors, is unable to account for various peculiarities in a wide range of temperatures and magnetic fields and, in particular, for transformations in the electronic and magnetic structure. Various experiments [1–5] reveal that the presence of doped magnetic moments in a strongly disordered semiconductor can combine features of the usual doping-driven metal–insulator transition in amorphous systems with the physics of the temperature- and field-driven magnetic (spin glass) transition. The competition between structural and magnetic disorder, which is responsible for the features observed at low temperatures in the magnetic and transport properties of a-RE_xSi_{1-x}, has been analyzed in Refs. [6, 7] within the framework of the Anderson–Mott transition driven by spin disorder. ESR and dc-magnetization results show (see Ref. [8]) that RE is incorporated as a trivalent ion (RE^{3+}) in the a-Si matrix. Two $(s-d)$ electrons of RE form saturated bonds with $(s-p)$ electrons of neighbored Si, while the third $(s-d)$ electron remains itinerant and participates in the conductivity; below, we consider RE as the one-electron donor in the amorphous silicon host.

So far, the a-RE_xSi_{1-x} alloy was considered as a completely disordered, heavily doped, magnetic semiconductor, and the role of the short-range structural and magnetic order was not discussed. However, as a rule, different kinds of disorder exist in such amorphous alloys [9]. The compositional disorder at the atomic scale distances, associated with dangling bonds, vacancies, and substitutional and interstitial centers, can be qualitatively described within a model of point defects

[*]E-mail: vvtugushev@mail.ru
[**]E-mail: chumakov@imp.kiae.ru

in a regular crystal lattice. The structural (topological) disorder at nanoscale distances, which is originated by dislocations or inclusions, has to be described in a different way, within a model of continuous defects with a short-range order, embedded into a completely disordered effective medium (matrix).

As we argue below, sharp spatial fluctuations of the RE concentration play an important role in a-RE_xSi_{1-x} in a wide temperature range, far above both the paramagnet–spin glass and the metal–insulator phase transitions (see, e.g., Ref. [9] for a discussion on the role of the so-called compositional disorder in amorphous semiconducting alloys). Experiments [1–5] revealed five distinct temperature regimes, characterized by different magnetic and transport properties. For instance, at $T > 70$ K, the temperature dependence of the electrical conductivity σ in a-Gd_xSi_{1-x} is similar to that of its nonmagnetic structural analogue a-Y_xSi_{1-x}. At $T < 50$–70 K, instead, a significant difference in their behavior has been observed, and the conductivity diminishes with decreasing temperature more rapidly in a-Gd_xSi_{1-x} than in a-Y_xSi_{1-x}. This fact points to the magnetic nature of the phenomenon. In the temperature range 5 K $< T <$ 50–70 K, the low-field magnetization qualitatively obeys the Curie–Weiss law, although with a small Curie constant and the effective temperature Θ; large negative magnetoresistance is found at $T < 50$ K. At $T < 5$ K, the material shows a spin-glass freezing. Samples that are metallic at high temperature show a tendency towards the metal–insulator transition at low temperature.

To explain these properties, the authors of Ref. [10] proposed that the strong structural disorder of the system favors the formation of clusters, i.e., nanoscale structural defects with an enhanced concentration of RE ions, leading to a redistribution of the electron density, such that regions with the higher electron density (electron «drops») appear within the a-RE_xSi_{1-x} matrix. Magnetic ordering inside the drops, more favorable than in the matrix, was predicted. To verify the magnetic state of the drops, a «local» experimental method, electron spin resonance (ESR), was proposed, together with conductivity and Hall-effect measurements. Preliminary ESR results were reported in Ref. [10] and allowed a rough estimate of some parameters of the drops. As is shown below, the typical radius of a drop for a-Gd_xSi_{1-x} is $r_D \approx 4.5$–6 Å, corresponding to the volume $v_D = 4\pi r_D^3/3 \approx 400$–800 Å^3; the number of RE ions inside a cluster is $\kappa_D \approx 10$–13; the volume fraction occupied by the drops is $f \approx 0.05$–0.1. The short-range ferromagnetic order inside the drops develops at a temperature $T \approx 100$ K and saturates in the temperature range 50 K $< T <$ 100 K; for 2–5 K $< T <$ 50 K, the magnetic moments of different drops are uncorrelated, but at $T <$ 2–5 K, they are frozen by a spin-glass transition in the matrix.

In this paper, we study the a-RE_xSi_{1-x} system in the temperature regime far above the metal–insulator and paramagnet–spin glass transitions, i.e., at $T \gg 2$–5 K for the a-Gd_xSi_{1-x} alloy. We describe the disordered amorphous magnetic semiconductor within a model similar to the one adopted in Refs. [6, 7], taking the short-range structural, electronic, and magnetic correlations into account in a semi-phenomenological way, within the so-called «local phase transition» approach [11]. To describe the effective electron potential and the charge and spin density distributions of electrons in the drops embedded into the a-RE_xSi_{1-x} matrix, we define the corresponding «order parameters». To obtain the ground-state electron density, we introduce a self-consistency equation in the form of a local electrical neutrality condition for an isolated drop. We also derive the criterion for a ferromagnetic instability and calculate the temperature of the «local» ferromagnetic transition inside a drop. Finally, we discuss some experimental findings on the behavior of the electrical conductivity as a function of temperature and magnetic field, and their correspondence to the predictions of our theory.

2. THE MODEL

a-RE_xSi_{1-x} alloys are systems with a rather complicated topological and compositional disorder. Itinerant electrons move in the crystal potential consisting of a periodic and a disordered part, the latter having components with very different characteristic length scales. Together with the local part, conventional for all amorphous alloys, provided by the potentials of Si dangling bonds and isolated RE ions included in the a-Si network, there is also a continuous part of the disordered potential. We suppose that it is formed in the vicinity of the RE clusters by the Coulomb «tails» of the potential of charged RE ions. Obviously, to make an analytic treatment possible, we need to simplify the real distribution of the crystal potential within some reasonable modeling, which we discuss in what follows.

We consider a set of structurally isolated clusters embedded into a weakly disordered matrix. The matrix is assumed quasi-homogeneous on length scales exceeding the inter-atomic distances, but small compared with the characteristic cluster size and the inter-cluster distance. We assume that the electron structure of

the matrix averaged over the realizations of the local random potential is qualitatively described in terms of quasi-periodic electron states with a finite lifetime. Following Ref. [9], we write the electron Hamiltonian of our system as a one-band model in the $\mathbf{k}-\mathbf{r}$ representation,

$$\mathcal{H} = \sum_{\mathbf{k},\alpha} E(\mathbf{k}) c^{\dagger}_{\mathbf{k},\alpha} c_{\mathbf{k},\alpha} + \\ + \int d\mathbf{r} \sum_{\alpha,\beta} \left[U_{\alpha\beta}(\mathbf{r}) + \Phi(\mathbf{r})\delta_{\alpha\beta}\right] \Psi^{\dagger}_{\alpha}(\mathbf{r}) \Psi_{\beta}(\mathbf{r}), \quad (1)$$

where $\mathbf{k} = -i\partial/\partial\mathbf{r}$ is the quasimomentum and $E(\mathbf{k})$ is the Bloch band dispersion of an ideal periodic lattice. The operator $c^{(\dagger)}_{\mathbf{k},\alpha}$ annihilates (creates) an electron in the Bloch state labeled by $\mathbf{k}$ with spin projection α, and the operator $\Psi^{(\dagger)}_{\alpha}(\mathbf{r})$ annihilates (creates) an electron at the point $\mathbf{r}$ with spin projection α.

The local part of the disordered potential has the form

$$U_{\alpha\beta}(\mathbf{r}) = \sum_i \left(\mathcal{V}\delta_{\alpha\beta} + \mathcal{J}\mathbf{S}_i \cdot \boldsymbol{\sigma}_{\alpha\beta}\right) \delta(\mathbf{r} - \mathbf{r}_i), \quad (2)$$

where $\mathcal{V}$ and $\mathcal{J}$ are the Coulomb and exchange couplings of the electrons with the impurities, respectively, $\mathbf{S}_i$ is the local spin vector, and $\boldsymbol{\sigma}$ is the vector of Pauli matrices. The sum in Eq. (2) ranges over the positions of the impurities located at the lattice sites $\mathbf{r}_i$, which are randomly distributed.

The continuous part of the potential is nonzero only inside the clusters and can be written as

$$\Psi(\mathbf{r}) = \sum_j \Phi_j(\mathbf{r}),$$

where $\Phi_j(\mathbf{r})$ is an effective «envelope» Coulomb potential of the jth cluster. In principle, the equation for $\Phi(\mathbf{r})$ has to be derived and solved self-consistently with the charge redistribution in the system. But in our model, for simplicity, we take $\Phi_j(\mathbf{r}) = \varphi$, independent of $\mathbf{r}$, inside the j-th cluster, and $\Phi_j(\mathbf{r}) = 0$ elsewhere. Within this simple approximation, φ occurs as a local shift of the bulk chemical potential μ inside a drop, $\mu_D = \mu + \varphi$.

To characterize the drops, we have to specify their properties. We let N_D and N_M denote the total number of RE ions in the clusters and in the matrix, respectively, with the total number of RE ions $N = N_D + N_M$ being fixed. The total volume occupied by the drops is V_D and the volume of the matrix is V_M, the total volume of the system $V = V_D + V_M$ being fixed. The volume fraction occupied by the drops is denoted by $f \equiv V_D/V < 1$. The RE ion density in the clusters is $n_D \equiv N_D/V_D = \gamma n$, where $\gamma > 1$ is the enhancement factor, and $n \equiv N/V$ is the nominal concentration of RE ions. Because $V_D = fV$, we have $N_D = f\gamma N$, $N_M = (1 - f\gamma)N$, and using $V_M = (1-f)V$, we can calculate the RE ion density in the matrix as

$$n_M \equiv \frac{N_M}{V_M} = \frac{1 - f\gamma}{1 - f}\, n.$$

To proceed further, we have to make some assumptions about the drops. For simplicity, we assume the drops to be equal and spherical, with the radius r_D and volume $v_D = 4\pi r_D^3/3$. The number of RE ions in a single cluster is then $\kappa_D = n_D v_D$ and the excess of RE ions with respect to the matrix is

$$\Delta\kappa \equiv (n_D - n_M)v_D = \frac{\gamma - 1}{1 - f}\,\kappa,$$

where $\kappa \equiv n v_D$ is the nominal number of RE ions in a single cluster. Thus, we have

$$\gamma = 1 + (1 - f)\frac{\Delta\kappa}{\kappa}, \quad (3)$$

and in what follows, we assume that $\Delta\kappa$ is a parameter of our model, which is possibly determined by the alloy growing conditions. It is related to the number of RE ions in a cluster by $\kappa_D = \gamma\kappa = \kappa + (1-f)\Delta\kappa$.

We still have to find a connection between f and v_D. Let $\mathcal{N}_D$ be the total number of drops. Then $fV = V_D = \mathcal{N}_D v_D$, i.e., $f = \mathcal{N}_D v_D/V$. Assuming that the number of drops per unit volume $\mathcal{N}_D/V$ is technologically fixed, we have that f is proportional to the volume of a drop v_D, i.e., to the nominal number of RE ions in a cluster, $\kappa = n v_D$. We write $f = \lambda\kappa$, with

$$\lambda \equiv \frac{\mathcal{N}_D}{N} = \frac{\mathcal{N}_D}{Vn}$$

viewed as a parameter. We must find a physical condition to determine κ, and hence all the drop parameters. As we show in Sec. 3A, this is the electrical neutrality condition for an isolated drop.

The potential φ, which determines the position of the local chemical potential in the drops $\mu_D = \mu + \varphi$, can be qualitatively estimated as an average electrostatic potential inside a drop of radius r_D,

$$\varphi = \frac{Ze^2}{\epsilon r_D}\,\Delta\kappa. \quad (4)$$

Here, e is the electron charge, we take the RE ion as a donor with the effective uncompensated positive charge $Z|e|$, and ϵ is the static dielectric constant of the system. For a-Gd_xSi_{1-x}, we have $Z = 1$ (see Sec. 1), $\epsilon \approx$ 12–15, the bandwidth of the itinerant electron

band is $W \approx 6$–8 eV, the average volume of the elementary cell is $a^3 \approx 20\,\text{Å}^3$, i.e., the average lattice spacing is $a \approx 2.7\,\text{Å}$. Thus, for a nominal chemical composition $x = 0.14$, the average concentration of RE ions is $n \approx 7 \cdot 10^{21}$ cm^{-3} [4, 5]. From the experimental results [10], we can estimate $\Delta\kappa \approx 7$–9, $\kappa \approx 3$–4, $\lambda \approx 0.01$–0.03. This gives the estimate $\mathcal{N}_D/V = f/v_D \approx (6\text{–}25) \cdot 10^{19}$ cm^{-3} for the number of drops per unit volume.

3. LOCAL DENSITY OF ELECTRON STATES AND BASIC EQUATIONS

In this section, we derive the equations that fix all the parameters of our model. We start by calculating the local density of states (DOS) in the matrix and in the drops, in the paramagnetic phase, through the usual expression [9] $\rho(\varepsilon) = \pi^{-1}\,\mathrm{Im}\langle G_A(\mathbf{r},\mathbf{r};\varepsilon)\rangle$, where ε is the electron energy and $G_A(\mathbf{r},\mathbf{r};\varepsilon)$ is the advanced one-particle Green's function associated with Hamiltonian (1), averaged over the realizations of disordered potential (2). Assuming that magnetic order is absent, i.e., $\langle \mathbf{S}_i \rangle = 0$ everywhere in the system, we obtain the expression

$$\rho(\varepsilon) = \mathrm{Im} \int_{-\infty}^{+\infty} \frac{\rho_0(z)}{\varepsilon - z - \Sigma_A(\varepsilon)} \frac{dz}{\pi}, \qquad (5)$$

where the energy ε is measured from the center of the band of the ideal lattice. The function $\rho_0(z)$ in Eq. (5) is the DOS corresponding to the electron spectrum $E(\mathbf{k})$ of the ideal lattice, and for definiteness, we adopt the semi-elliptic form

$$\rho_0(z) = \begin{cases} \dfrac{2}{\pi}\sqrt{1-z^2}, & |z| \le 1, \\ 0, & |z| > 1. \end{cases} \qquad (6)$$

We take energy and length units such that half the bandwidth $W/2$ and the size of the elementary cell a are equal to one. The advanced self-energy $\Sigma_A(\varepsilon)$ is obtained by averaging over the realizations of the disordered potential $U(\mathbf{r})$ in Eq. (2) within some approximation scheme. As is customary, we include the average $\langle U(\mathbf{r})\rangle$ into the chemical potential μ; if we then assume that the impurities giving rise to the random potential in Eq. (2) are uncorrelated over different impurity sites $\mathbf{r}_i$, we find $\langle [U(\mathbf{r})]^2\rangle = [\mathcal{V}^2 + S(S+1)\mathcal{J}^2] n_{imp}$ in the noncrossing Born approximation, where n_{imp} is the concentration of impurities. Explicit results for $\Sigma(\varepsilon)$ were obtained in Refs. [6, 7] by means of numerical calculations for different values of the scattering parameter $\langle [2U/W]^2\rangle$. For our qualitative purposes, it is sufficient to assume that the fluctuations of potential (2) lead to a simple homogeneous broadening of the ideal semi-elliptic DOS (6), with a finite inverse lifetime 2Γ proportional to the scattering parameter. Thus, the resulting local DOS in our model is characterized by a tail of localized states (see Fig. 1). Using Eq. (5) with $\Sigma_A(\varepsilon) = i\Gamma$ and with $\rho_0(z)$ given by Eq. (6), we find

$$\rho(\varepsilon) = \frac{2}{\pi}\left(\sqrt{\sqrt{\mathcal{R}^2 + \varepsilon^2\Gamma^2} - \mathcal{R}} - \Gamma\right), \qquad (7)$$

where $\mathcal{R} \equiv (\varepsilon^2 - \Gamma^2 - 1)/2$.

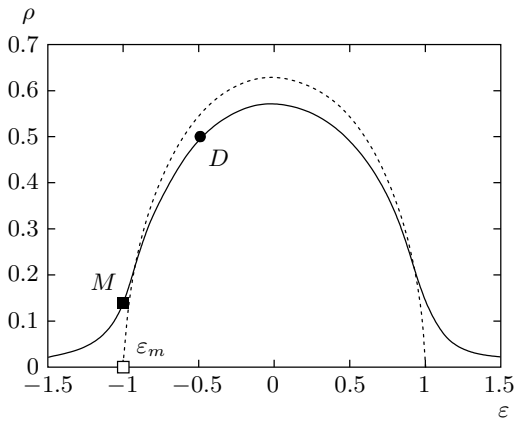

Fig. 1. Dashed line: the semi-elliptic DOS, Eq. (6), of the ideal lattice. Solid line: the DOS resulting from the inclusion of «local» impurity effects, resulting in a broadening of the semi-elliptic DOS, Eq. (7), with $\Gamma = 0.1$. The empty square marks the position of the mobility edge assumed at the bottom of the ideal band, $\varepsilon_m = -1$. The black square, labeled by M, and the black circle, labeled by D, mark the value of the DOS in the matrix and in the drops, respectively, for the set of parameters adopted in the text

A. The paramagnetic phase

We start our analysis by discussing the properties of the paramagnetic phase. Hereafter, the subscript p indicates that the corresponding quantity is evaluated in the paramagnetic phase, whenever this is expected to have a different value in the phase with a short-range ferromagnetic order, discussed in Sec. 3B.

The chemical potential of the system in the paramagnetic phase, μ_p, is fixed by the condition of conservation of the average number of electrons,

$$2(1-f_p)\int\limits_{-\infty}^{+\infty}\rho(\varepsilon)f(\varepsilon-\mu_p)\,d\varepsilon + 2f_p\int\limits_{-\infty}^{+\infty}\rho(\varepsilon)f(\varepsilon-\mu_p-\varphi_p)\,d\varepsilon = x, \quad (8)$$

where the factors 2 account for the spin degeneracy, $f_p = \lambda\kappa_p$ is the volume fraction occupied by the drops in the paramagnetic phase, $f(z) = [\exp(z/T)+1]^{-1}$ is the Fermi–Dirac distribution function at the temperature T (in energy units), and $x = na^3$ is the nominal RE content of the alloy (here, RE ions are taken as donors with $Z = 1$, such that the number of doped electrons in the conduction band equals the number of RE ions). For simplicity, we assume that the inverse lifetime Γ is the same in the matrix and in the drops, although this assumption plays no role in the following derivation, and we could even adopt a different DOS $\rho_{M,D}(\varepsilon)$ in the matrix and in the drops.

As discussed in Sec. 2, the excess of RE ions inside a cluster, $\Delta\kappa$, causes an increase of the electron density with respect to the matrix, which is controlled by the average potential φ_p in Eq. (4) with $r_D \to r_{D,p}$ in the paramagnetic phase. We assume that the electrical neutrality condition is satisfied for an isolated drop, ensuring that the excess of the RE ion density is screened by the corresponding excess of the electron density,

$$2\int\limits_{-\infty}^{+\infty}\rho(\varepsilon)f(\varepsilon-\mu_p-\varphi_p)\,d\varepsilon = \gamma_p x, \quad (9)$$

where γ_p is the density enhancement factor, Eq. (3), calculated in the paramagnetic phase (i.e., with $f \to f_p$, $\kappa \to \kappa_p$). With Eq. (9), we can rewrite Eq. (8) in the simpler form

$$2\int\limits_{-\infty}^{+\infty}\rho(\varepsilon)f(\varepsilon-\mu_p)\,d\varepsilon = (1-\lambda\Delta\kappa)x, \quad (10)$$

whence it is evident that the chemical potential μ_p is uniquely determined in terms of the parameters of our model. Once μ_p is obtained form Eq. (10), Eq. (9) contains κ_p (or, equivalently, $r_{D,p}$) as the only variable, and can be easily solved by means of standard numerical methods.

The simultaneous numerical solution of Eqs. (9) and (10) at $T = 0$, e.g., for $x = 0.14$, $W = 8$ eV, $\epsilon = 12$, $\Delta\kappa = 9$, and $\lambda \approx 0.029$, with $\Gamma \approx 0.1$ (chosen as in Refs. [6, 7] to fix the chemical potential at the mobility edge, $\mu_p = -1$, see below) yields $\kappa_p \approx 3.1$, which gives $f_p \approx 0.091$ and $\gamma_p \approx 3.34$. Hence, the number of RE ions in a cluster is $r_{D,p} \approx 10.4$, the volume of a drop is $v_{D,p} \approx 440\,\text{Å}^3$, and the radius of a drop is $r_{D,p} \approx 4.7\,\text{Å}$. The value of the Coulomb shift of the chemical potential in the drops is $\varphi_p \approx 0.51$ (which corresponds to an energy approximately 2 eV). The local DOS at the Fermi level is $\rho(\mu_p) \approx 0.14$ and $\rho(\mu_p+\varphi_p) \approx 0.50$ in the matrix and in the drops, respectively (the maximum value for the DOS is $\rho_{max} \approx 0.58$ for the chosen set of parameters, see Fig. 1).

So far, we have discussed only the paramagnetic phase of the system, and hence our results are valid for both the magnetic alloy a-Gd_xSi_{1-x} (at $T > T_D$, see Sec. 3B) and the nonmagnetic alloy a-Y_xSi_{1-x}.

For small f_p, well below the percolation limit of the drops, the electron states within the drops are localized in the volume v_D and are separated from the matrix by a surface energy barrier, which determines the excitation energy of a drop, $\mathcal{E}_D$. Also the electron states within the tail of the DOS of the matrix are localized at the scale of inter-atomic distances. Therefore, at $T \ll \mathcal{E}_D$, the fraction of itinerant electrons within the elementary cell in our system can be estimated as

$$x_{itin,p} = 2(1-f_p)\int\limits_{\varepsilon_m}^{+\infty}\rho(\varepsilon)f(\varepsilon-\mu_p)\,d\varepsilon, \quad (11)$$

where ε_m is the mobility edge, which depends on the scattering potential. We assume, for simplicity, that it is located at the bottom of the ideal lattice band, $\varepsilon_m = -1$. Although, strictly speaking, one should define the position of the mobility edge self-consistently, from the calculation of the two-particle Green's function of the system, our simplifying assumption does not play a relevant role.

The variation of $x_{itin,p}$ with increasing temperature in the paramagnetic phase, together with tiny variation of the chemical potential μ_p and of the Coulomb shift φ_p, is reported in Fig. 2 for the chosen set of parameters. As can be noticed, because the Fermi level was fixed at the mobility edge at $T = 0$, the itinerant electrons are thermally excited from the localized states in the tails of the DOS at finite temperature, and their density increases almost linearly with T. We note that $x_{itin,p}$ is at most about $0.006x$ at the highest temperature reported in Fig. 2 (which corresponds to $T \approx 200$ K), and therefore itinerant electrons are a tiny fraction of all the electrons in the system, the most part being localized into the DOS tails. Therefore, whereas the nominal density of doped electrons is $n \approx 7\cdot 10^{21}$ cm^{-3}, the density of thermally excited itinerant electrons is, e.g., $n_{itin,p} \approx 4\cdot 10^{19}$ cm^{-3} at $T \approx 200$ K.

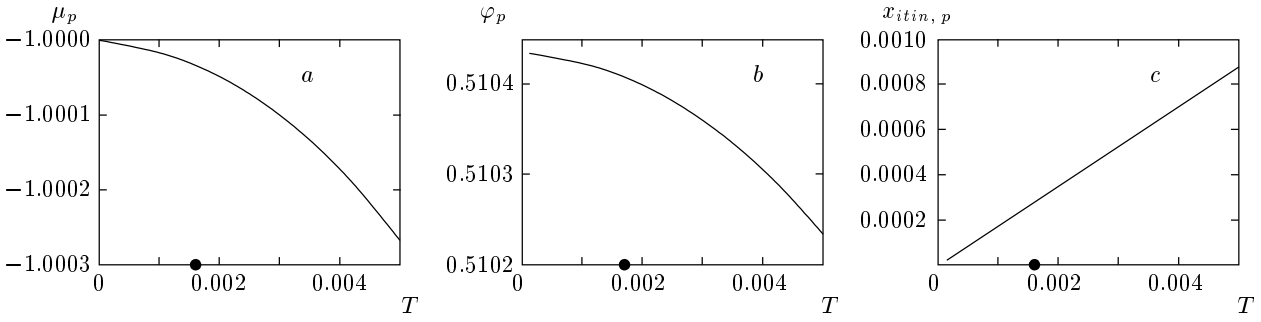

Fig. 2. *a*) Temperature dependence of the chemical potential μ_p in the paramagnetic phase as resulting from the numerical solution of Eq. (10) at finite temperature. *b*) Temperature dependence of the Coulomb shift φ_p in the paramagnetic phase as resulting from the numerical solution of Eq. (9) at finite temperature and with $\mu_p(T)$ previously determined. *c*) Temperature dependence of the fraction of itinerant electrons in the paramagnetic phase, $x_{itin,p}$, calculated according to Eq. (11). In all the three panels, the black circle on the temperature axis marks the transition point to the phase with a short-range ferromagnetic order in the drops

B. The phase with a short-range ferromagnetic order

In this section, we treat the exchange part of Hamiltonian (1) in the mean-field approximation, supposing $\langle \mathbf{S}_i \rangle = 0$ in the matrix and $\langle \mathbf{S}_i \rangle \neq 0$ inside the drops. This assumption is quite reasonable in a wide temperature range, because the local DOS at the Fermi level is larger in the drops than in the matrix (see Fig. 1), and therefore the condition for ferromagnetic ordering in the presence of an exchange coupling between magnetic RE ions and electrons is more easily realized in the drops. The magnetic RE ions inside the clusters experience the effective magnetic field

$$H_{eff} = \mathcal{J} \int_{-\infty}^{+\infty} [\rho(\varepsilon + m) - \rho(\varepsilon - m)] \times \\ \times f(\varepsilon - \mu - \varphi)\, d\varepsilon, \quad (12)$$

where $m \equiv \mathcal{J} x_D \langle S_z \rangle$, $x_D = \gamma x$ is the concentration of magnetic (e.g., Gd) RE ions per unit cell in a cluster, the index z defines the direction of the local quantization axis, and the average value of the spin at the RE site is defined self-consistently as

$$\langle S_z \rangle = S \mathcal{B}_S \left(\frac{S H_{eff}}{T} \right),$$

where

$$\mathcal{B}_S(y) = \frac{2S+1}{2S} \operatorname{ch}\left(\frac{2S+1}{2S}\, y \right) - \frac{1}{2S} \operatorname{ch}\left(\frac{1}{2S}\, y \right)$$

is the Brillouin function for spin S. For Gd ions, $S = 7/2$.

The above equations should be solved simultaneously, together with the equation for the chemical potential μ,

$$2(1-f) \int_{-\infty}^{+\infty} \rho(\varepsilon) f(\varepsilon - \mu)\, d\varepsilon + \\ + f \int_{-\infty}^{+\infty} [\rho(\varepsilon+m) + \rho(\varepsilon-m)]\, f(\varepsilon - \mu - \varphi)\, d\varepsilon = x, \quad (13)$$

which corresponds to the conservation of the average number of electrons in the phase with a short-range ferromagnetic order within the drops, and the equation for κ, which enforces charge neutrality for an isolated drop,

$$\int_{-\infty}^{+\infty} [\rho(\varepsilon + m) + \rho(\varepsilon - m)]\, f(\varepsilon - \mu - \varphi)\, d\varepsilon = \gamma x, \quad (14)$$

where γ is the density enhancement factor defined in Eq. (3). As discussed above, we assume that the number of excess RE ions $\Delta\kappa$ does not change in passing from the paramagnetic phase to the phase with a short-range ferromagnetic order, whereas the radius of the drops changes from $r_{D,p}$ to r_D (i.e., the nominal number of RE ions within the clusters changes from κ_p to κ). The volume fraction occupied by the drops is $f = \lambda\kappa$, where λ is the same as in the paramagnetic phase, assuming that the number of drops per unit volume does not change across the local ferromagnetic transition.

Using Eq. (14), we can rewrite Eq. (13) as

$$2\int\limits_{-\infty}^{+\infty}\rho(\varepsilon)f(\varepsilon-\mu)\,d\varepsilon=(1-\lambda\Delta\kappa)x, \qquad (15)$$

which concides with Eq. (10). Therefore, it is evident that for a given set of parameters, the chemical potential has the same value as in the paramagnetic phase at the same temperature, $\mu(T)=\mu_p(T)$.

The typical value of the exchange potential in the units of $W/2$ is $\mathcal{J}S \approx 0.1$–$0.2 \ll \varphi$. In what follows, we take m as a small expansion parameter and seek solutions of the above self-consistency equations that are close to the solutions in the paramagnetic phase, $r_D = r_{D,p} + \eta$, with $\eta \ll r_{D,p}$. We observe that $\varphi \approx \varphi_p - e^2\Delta\kappa\eta/\epsilon r_{D,p}^2 \equiv \varphi_p + \zeta$, with $\zeta \equiv -\eta\varphi_p/r_{D,p} \ll \varphi_p$. The volume of a drop changes as $v_D \approx v_{D,p}(1+3\eta/r_{D,p})$, and hence $\kappa = nv_D \approx \kappa_p(1+3\eta/r_{D,p})$, $f=\lambda\kappa \approx f_p(1+3\eta/r_{D,p})$, and $\gamma \approx \gamma_p(1+3\Delta\kappa\eta/\gamma_p\kappa_p r_{D,p})$.

Now, we expand the DOS and the Fermi–Dirac distribution function as

$$\rho(\varepsilon+\sigma m)\approx\rho(\varepsilon)+\rho'(\varepsilon)\sigma m+\frac{1}{2}\rho''(\varepsilon)m^2+ \\ +\frac{1}{6}\rho'''(\varepsilon)\sigma m^3 \quad (\sigma=\pm1),$$

$$f(\varepsilon-\mu_p-\varphi)\approx f(\varepsilon-\mu_p-\varphi_p)-f'(\varepsilon-\mu_p-\varphi_p)\zeta$$

(here and in what follows, the prime is a short notation for the derivative with respect to ε). Then Eq. (14) for charge neutrality, at this order of approximation, gives

$$-2\left[\int\limits_{-\infty}^{+\infty}\rho(\varepsilon)f'(\varepsilon-\mu_p-\varphi_p)\,d\varepsilon\right]\zeta+ \\ +\left[\int\limits_{-\infty}^{+\infty}\rho''(\varepsilon)f(\varepsilon-\mu_p-\varphi_p)\,d\varepsilon\right]m^2=\frac{3x\Delta\kappa}{\kappa_p\varphi_p}\,\zeta, \qquad (16)$$

i.e., $L\zeta + Mm^2 = 0$, where the coefficients L and M are calculated in the paramagnetic phase. The coefficient M is reexpressed in a more suitable form via integration by parts that transfers the derivative with respect to ε from ρ to the Fermi–Dirac distribution function f. At low temperature $T \ll \varphi_p$, we find $L = 2\rho(\mu_p+\varphi_p) - (3x\Delta\kappa/\kappa_p\varphi_p)$ and $M=\rho'(\mu_p+\varphi_p)$.

It is evident that $\zeta \sim m^2$, as expected, because corrections to the Coulomb shift cannot depend on the sign of the magnetization. Finally, expression (12) for the effective field up to $O(m^3)$ becomes

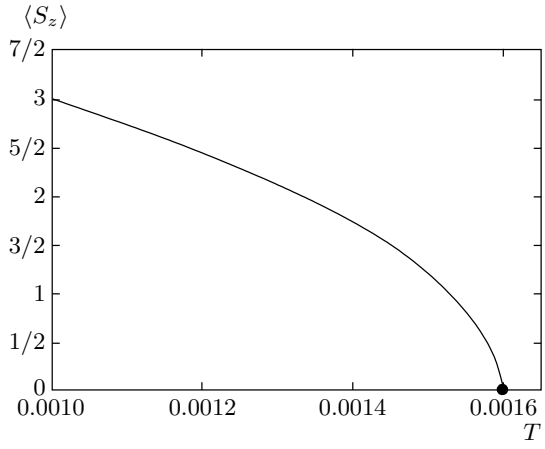

Fig. 3. Temperature dependence of the magnetization of a Gd ion in a cluster, $\langle S_z\rangle \equiv m/\mathcal{J}x_D$, obtained by solving Eq. (18) for T close to T_D. The values of the parameters are given in the text. The local transition point at $T=T_D=0.0016$ is marked by a black circle

$$H_{eff}\approx 2\mathcal{J}\left[\int\limits_{-\infty}^{+\infty}\rho'(\varepsilon)f(\varepsilon-\mu_p-\varphi_p)\,d\varepsilon\right]m+ \\ +\frac{\mathcal{J}}{3}\left[\int\limits_{-\infty}^{+\infty}\rho'''(\varepsilon)f(\varepsilon-\mu_p-\varphi_p)\,d\varepsilon\right]m^3- \\ -2\mathcal{J}\left[\int\limits_{-\infty}^{+\infty}\rho'(\varepsilon)f'(\varepsilon-\mu_p-\varphi_p)\,d\varepsilon\right]m\zeta,$$

i.e., $H_{eff} \approx Am + Bm^3 + Cm\zeta$, where the coefficients A, B, and C are calculated in the paramagnetic phase. The coefficients A and B are reexpressed in a more appropriate form via integration by parts that transfers the derivative with respect to ε from ρ to f. At low temperature, $A = 2\mathcal{J}\rho(\mu_p+\varphi_p)$, $B=\mathcal{J}\rho''(\mu_p+\varphi_p)/3$, and $C = 2\mathcal{J}\rho'(\mu_p+\varphi_p) = 2\mathcal{J}M$.

We find the solution of Eqs. (12)–(15) near the «local phase transition», i.e., at temperatures close to the local Curie point of the drops T_D (which is defined below), where our expansion in powers of m and ζ is valid. We must expand the Brillouin function, observing that $\mathrm{ch}(y) \approx 1/y + y/3 - y^3/45$, i.e.,

$$\mathcal{B}_S(y)\approx\frac{S+1}{3S}\,y-\frac{2S^3+(2S+1)^2}{90S^3}\,y^3.$$

Then, the self-consistency equation for m in the phase with a short-range ferromagnetic order for $T \lesssim T_D$ (T_D is defined below), at the same order of approximation, becomes

$$1 = \mathcal{J} x \gamma_p S \left\{ \frac{S+1}{3T} \left[A + Bm^2 + (C+D)\zeta \right] - \right.$$
$$\left. - \frac{2S^3 + (2S+1)^2}{90T^3} A^3 m^2 \right\}, \quad (17)$$

where $D = 3A\Delta\kappa/\gamma_p\kappa_p\varphi_p$ accounts for the variation of γ (i.e., of $x_D = x\gamma$) in entering the phase with the short-range ferromagnetic order. Equation (17) must be solved together with Eq. (16) to yield ζ and m^2.

It is evident that the local transition temperature for the drops is $T_D = \mathcal{J}A^*S(S+1)/3$, where $A^* \equiv Ax\gamma_p = Aa^3\kappa_D/v_D$. We note that in our simple mean-field approach and within the approximation of isolated drops, the full dependence of the transition temperature T_D on the mean RE concentration x might not be correctly described, because κ_D and v_D are the local parameters of a drop, which within our model are self-consistently determined by x and by the cluster parameters $\Delta\kappa$ and λ, assumed fixed. A more developed theory has to account for both charge and spin correlations in the system (which may introduce a dependence of $\Delta\kappa$ and λ on x), as well as an exchange between moments of different drops, to describe the correct dependence of T_D on x. However, this quantitative description is beyond the scope of our paper.

For $T > T_D$, Eq. (17) has no real solutions and $m = 0$. For $T < T_D$, the ferromagnetic solution within the drops becomes stable. From Eq. (16), we find $\zeta = -Mm^2/L$, and substituing this in Eq. (17), we obtain the equation for m^2 for $T \lesssim T_D$,

$$m^2 = \frac{\frac{1}{3}\mathcal{J}Ax\gamma_p S(S+1) - T}{\mathcal{J}x\gamma_p S\left[(S+1)\frac{M(C+D) - BL}{3L} + \frac{2S^3 + (2S+1)^2}{90T^2} A^3\right]} \equiv \frac{T_D - T}{P + \frac{Q}{T^2}} \approx \frac{T_D - T}{P + \frac{Q}{T_D^2}}, \quad (18)$$

where P and Q are constants, which depend on the parameters calculated in the paramagnetic phase, and whose expression can be easily deduced from Eq. (18). For a-$Gd_{0.14}Si_{0.86}$, we have $\rho'(\mu_p + \varphi_p) \approx 0.35$, $\rho''(\mu_p + \varphi_p) \approx -0.91$, and taking $\mathcal{J} \approx 0.026$ (which corresponds to the energy 0.1 eV, a typical exchange energy in wide-band magnetic semiconductors), we find $T_D = 0.0016$ (which corresponds to the temperature 70 K) and $P + Q/T_D^2 \approx 0.45$. The magnetization of the magnetic RE ions within the clusters, $\langle S_z \rangle = m/\mathcal{J}x_D \approx m/\mathcal{J}x\gamma_p$, near the local transition point T_D is reported in Fig. 3.

We point out that our results are correct only within the mean-field approximation for the RE spin density. The finite volume of the drops causes a «tail» of fluctuations of the magnetization to occur at $T > T_D$, in the temperature range $(T - T_D)/T_D \sim (r_D/a)^{-2} \approx 0.1$–$0.2$.

4. EXPERIMENTS AND DISCUSSION

The X-ray study of the local structure of a-Gd_xSi_{1-x} revealed a strong local distortion of the matrix around Gd ions, as well as the absence of fluctuations on macroscopic scales in the system [12]. Detailed conductivity and tunneling measurements revealed the coexistence of metallic and semiconducting domains (micro- or meso-scopic), identifying the percolation nature of electron transport at low temperatures, near the metal–insulator transition [13]. Here, we consider some interesting experimental results, obtained at temperatures far above the metal–insulator transition, and discuss their correspondence to the predictions of our theory. The results are obtained using the samples prepared in Prof F. Hellman's laboratory by a technique described previously [2]. Amorphous films of a-$(Gd,Y)_xSi_{1-x}$, 100–500 nm thick, were grown by e-beam coevaporation on Si/SiN substrates. Magnetotransport measurements were carried out in the temperature range 5–300 K in magnetic fields up to 4 T using the Van der Pauw and standard Hall bar technique.

Experiments [1–5] have clearly shown that the electrical conductivity σ increases almost linearly with the temperature T in a-Y_xSi_{1-x} at $T > 2$–5 K and in a-Gd_xSi_{1-x} at $T > 50$–70 K. This dependence is well described by the expression

$$\sigma_p(T) \approx \sigma_0 + \sigma_{itin,p}(T) \quad (19)$$

where σ_0 is constant and $\sigma_{itin,p}(T)$ depends on the temperature. To explain these results, we propose that in a-RE_xSi_{1-x} alloys, the electrically neutral drops play a significant role in the itinerant electron transport. The constant part σ_0 is associated with the tunneling between the drops and the matrix through the surface barrier, while $\sigma_{itin,p}(T) = x_{itin,p}(T)\nu_p(T)$, where $\nu_p(T)$ is the itinerant electron mobility in the paramagnetic state. To clarify the role of the itinerant electron concentration in the temperature dependence of the electrical conductivity, Hall effect measurements were carried out.

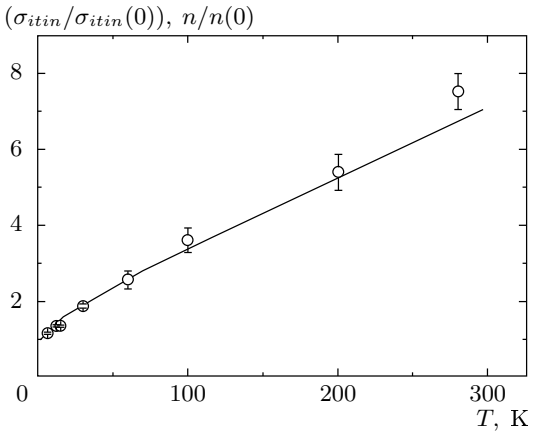

Fig. 4. Temperature dependence of the itinerant electron conductivity (solid line) and concentration (open circles) for the nonmagnetic $Y_{0.17}Si_{0.83}$ sample

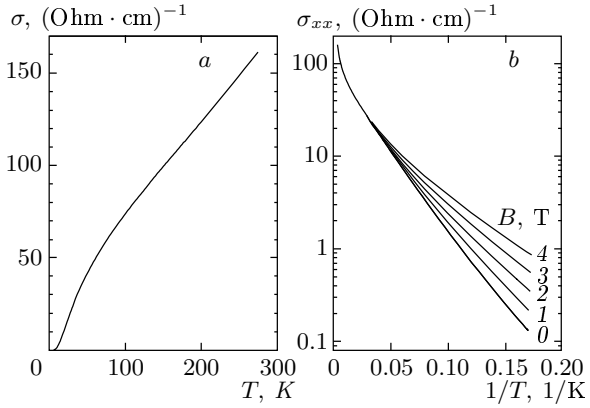

Fig. 5. *a*) Conductivity vs temperature dependence for the $Gd_{0.135}Si_{0.865}$ sample № 5 at zero magnetic field. *b*) Conductivity vs $1/T$ at various magnetic fields, for the same sample

In Fig. 4, we present the experimentally determined itinerant electron concentration $n(T)$ for nonmagnetic a-Y_xSi_{1-x}, which linearly increases with temperature in the whole temperature range. According to our model, this implies that the dependence of $\nu_p(T)$ on T is weak enough, as resulting from the scattering of itinerant electrons on electrically neutral centers. The temperature dependence of the itinerant electron electrical conductivity presented in Fig. 4 is build by taking into account some shunting tunneling conductivity σ_0, which does not contribute to the Hall effect. The data show that $\sigma_{itin,p}(T)/\sigma_{itin,p}(0) \approx n(T)/n(0)$ and confirm that the variation of $\sigma_{itin,p}(T)$ is produced by $n(T)$, which increases linearly with T.

For the a-Gd_xSi_{1-x} magnetic alloys, the increase of $\sigma_p(T)$ with T is strongly nonlinear at T below approximately 50–70 K and becomes quasilinear only above this temperature (see Fig. 5). We attribute this nonlinearity to complex magnetic transformations in the system. Consistently with the theory developed in Sec. 2, for $T < T_D \approx 50$–70 K, when the short-range ferromagnetic order is formed in the alloys containing magnetic RE atoms, two factors modify the temperature dependence of the conductivity $\sigma(T)$.

First, there occurs the exchange scattering of electrons on the noncorrelated magnetic moments of the drops, which shifts the mobility edge ε_m in Eq. (11) upwards,

$$\frac{\Delta\varepsilon_m}{\Gamma} \sim \beta(T) \equiv \frac{\lambda\left(\mathcal{J}\kappa_D\langle S_z\rangle\right)^2}{\mathcal{V}^2},$$

thus decreasing the concentration of itinerant electrons in the phase with a short-range ferro-magnetic order, $x_{itin}(T)$.

Second, a dependence of the mobility $\nu(T)$ of the itinerant electrons on T appears, which is qualitatively described as a superposition of the potential and exchange mechanisms for electron scattering on the disordered magnetic drops with a characteristic size that is small compared to the electron mean free path, $\nu(T)/\nu_p(T) \sim 1 - \beta(T)$. Thus, the reduction of $\sigma(T)$ with decreasing temperature is driven, in principle, by both mechanisms.

The parameter $\beta(T)$ is zero at $T > T_D$ and may be of the order 0.01–0.1 at $T \ll T_D$ if $\mathcal{J}S/\mathcal{V} \approx 0.1$–0.3, $\kappa_D \approx 10$–12, and $\lambda \approx 0.01$–0.03. From the data in Fig. 5, we conclude that the variation of the itinerant electron concentration plays the major role in our system, and the variation of the itinerant electron mobility can be neglected in the following discussion. In any case, the appearance of a short-range ferromagnetic order obviously enhances the tendency towards the metal–insulator transition.

We briefy discuss the variation of the conductivity σ of our system as a function of the temperature and of the external magnetic field $\mathbf{B}$. At $T < 50$–70 K, a strong exponential dependence of the conductivity on the temperature (see Fig. 5*b*) and on the magnetic field (see Fig. 6) is observed. There are two regimes of magnetic fields characterized by a different behavior of $\sigma(B)$. In a magnetic field less than some critical value B_C, the conductivity slightly depends on the magnetic field. At $B > B_C$, the aforementioned exponential dependence of σ on B is observed (see Fig. 6*b*); the critical value B_C increases with increasing temperature (see

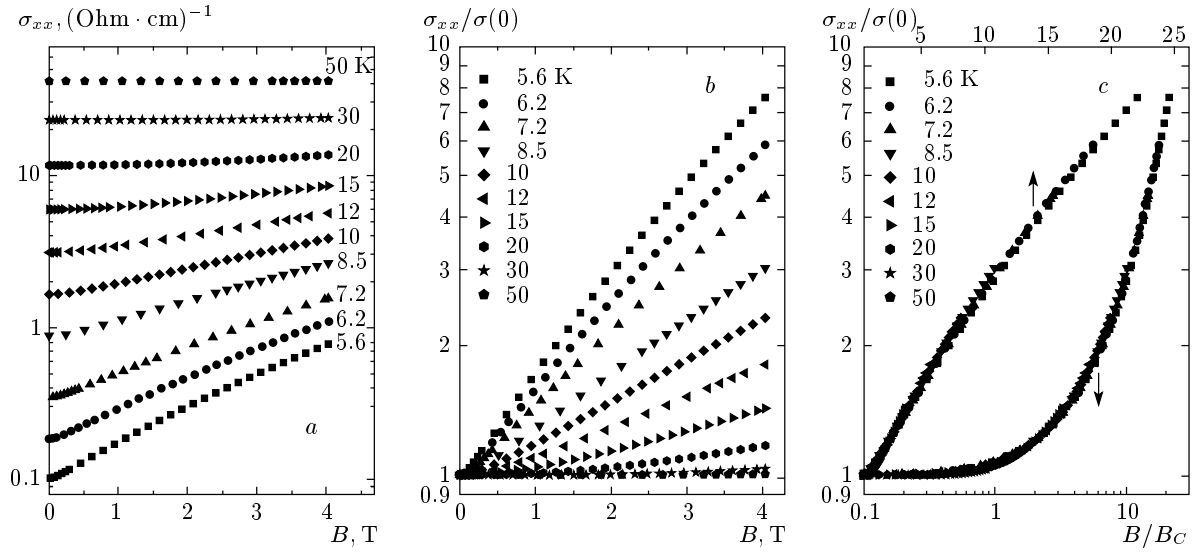

Fig. 6. *a*) Conductivity vs magnetic field dependence for the $Gd_{0.135}Si_{0.865}$ sample № 5 at different temperatures. *b*) The same dependence when the conductivity is rescaled by the zero-field vale $\sigma(0)$. *c*) The same dependence when the magnetic field is rescaled by the critical value B_C, which evidences the data collapse

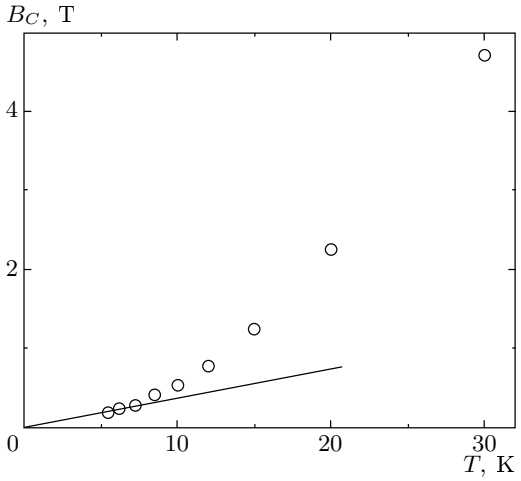

Fig. 7. Temperature dependence of the critical magnetic field B_C for the $Gd_{0.135}Si_{0.865}$ sample № 5

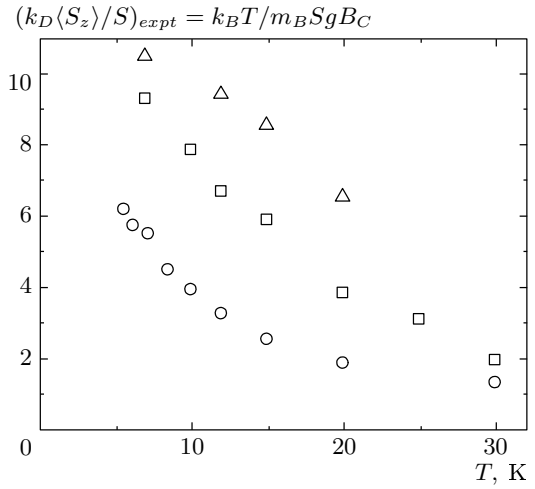

Fig. 8. Temperature dependence of the mean magnetic moment of the clusters for the $Gd_{0.135}Si_{0.865}$ sample № 5 (open circles), for the $Gd_{0.14}Si_{0.86}$ sample № 3 (open squares), and for the $Gd_{0.145}Si_{0.855}$ sample № 7 (open triangles)

Fig. 7). B_C is determined by the intersection of the local fit of the experimental $\log[\sigma/\sigma(0)]$ as a function of B with the line $\sigma/\sigma(0) = 1$ at low temperatures. For high temperatures, B_C is the scaling parameter from Fig. 6*c*. We suppose that B_C corresponds to the critical magnetic field that aligns the magnetic moments of the drops. At low magnetic field, the magnetic energy of the drop $\kappa_D\langle S_z\rangle m_B gB$ (here, m_B is the Bohr magneton and g is the gyromagnetic ratio) is smaller than the thermal energy k_BT and the magnetic moments of different drops are disordered. This leads to an additional fluctuation potential in the system and raises the mobility edge. Magnetic fields larger than B_C align the magnetic moments of different drops and eliminate this scattering channel. This reduces the mobility edge and increases the itinerant electron concentration, leading to an increase in the conductivity.

It is important that the value of the magnetic moment of the drop obtained from the low-temperature part of the curve $B_C(T)$ allows us to estimate the average number of Gd atoms in the cluster, κ_D. The experimentally determined value of $(\kappa_D\langle S_z\rangle/S)_{expt} = k_BT/m_BSgB_C$ is shown in Fig. 8. At low T, when $\langle S_z\rangle \approx S$, we obtain $\kappa_{D,expt} \approx 10$, which is consistent with the prediction of our theory. The experimentally determined κ_D values are close for different samples. We suppose that if the clusters arise during the sample growth, their size may depend on the synthesis conditions.

We note that the magnetic-field dependence of the conductivity has a universal form for different temperatures. The experimental dependences of $\sigma/\sigma(0)$ vs. (B/B_C) (here, $\sigma(0)$ is the zero-field conductivity) for different temperatures are presented in Fig. 6*c*. The experimentally observed behavior of $\sigma/\sigma(0)(B/B_C)$ obeys the law

$$\frac{\sigma}{\sigma(0)} \approx \exp\left(\frac{B}{B_C} - 1\right), \tag{20}$$

at $B > B_C$, where $B_C = k_BT/M$ and $M = m_B\langle S_z\rangle g\kappa_{D,expt}$. At $B \gg B_C$, this gives

$$\frac{n}{n(0)} \approx \exp\left(\frac{B}{B_C}\right), \tag{21}$$

where n ($n(0)$) is the density of itinerant electrons (at zero field). Our explanation of this result is as follows. We suppose that the Zeeman splitting in the matrix leads to a downward (upward) shift of the bottom of the itinerant electron spin-up (spin-down) subband with respect to the Fermi level. At high B, the full splitting regime sets in when the spin-down sub-band remains empty, the local Fermi energy measured from the bottom of the spin-up subband rises linearly with B, and the itinerant electron concentration increases according to Eq. (11).

Our experiments as well as previous data [1–5] have shown that the application of a strong magnetic field B suppresses the tendency towards the metal–insulator transition and even induces an insulator-to-metal transformation in some a-RE_xSi_{1-x} alloys with low RE concentration. This fact is naturally explained within our model, if we take into account either the increase of the itinerant electron concentration or the suppression of the electron exchange scattering on the magnetic drops provided by their coherent orientation in the magnetic field.

What is an external influence, besides the magnetic field, that may increase the itinerant electron concentration in the studied system? A way to vary the electron concentration is to increase the current I through the sample. To provide a more uniform current density distribution over the sample, we have used the standard Hall bar geometry of measurements. The conductance G and relative conductivity $\sigma/\sigma(0)$ dependences on the current at different temperatures are presented in Fig. 9, where σ ($\sigma(0)$) is the conductivity (at zero current limit). (G is used because of the small sample size and not well-defined geometrical factor for σ calculation.) We note that these dependences are analogous to such dependences vs. magnetic field, shown in Fig. 10. These figures clearly demonstrate that the current effect on the system is analogous to the influence of the external magnetic field. We suppose that a current flow I through the sample enhances the effective exchange between the magnetic moments of disordered drops, because it increases the itinerant electron concentration. If I exceeds some critical value I_C, determined by the same procedure as B_C, all the drops on the percolation path become magnetically ordered, which leads to a suppression of the fluctuation potential of the magnetic disorder. Increasing the current also leads to the rise of the itinerant electron concentration and to the reduction of the activation energy between the Fermi level and the mobility edge, which is consistent with Eq. (11).

5. CONCLUSION

We presented the theoretical description and electrical conductivity measurements for amorphous a-$(Gd,Y)_xSi_{1-x}$ alloys with $0.1 < x < 0.2$. We took the strong topological disorder in the system into account: in our approach, the nanoscale structural defects, enriched with rare-earth ions («clusters»), cause the appearance of regions with higher electron density (electron «drops»). The value of the local DOS at the Fermi level in the drops significantly exceeds the value of the DOS at the Fermi level in the matrix, and therefore a short-range ferromagnetic order appears in the drops below some characteristic temperature T_D. We estimated T_D in the «local phase transition» approach and analyzed measurements of the temperature and magnetic-field dependence of the electrical conductivity in amorphous $(Gd,Y)_xSi_{1-x}$ alloys, in the framework of the drop description. We obtained a qualitative agreement between the experimental results and the theoretical predictions. Further ESR measurements, scanning electron microscopy with polarization analysis (SEMPA) and neutron diffraction (ND) experiments

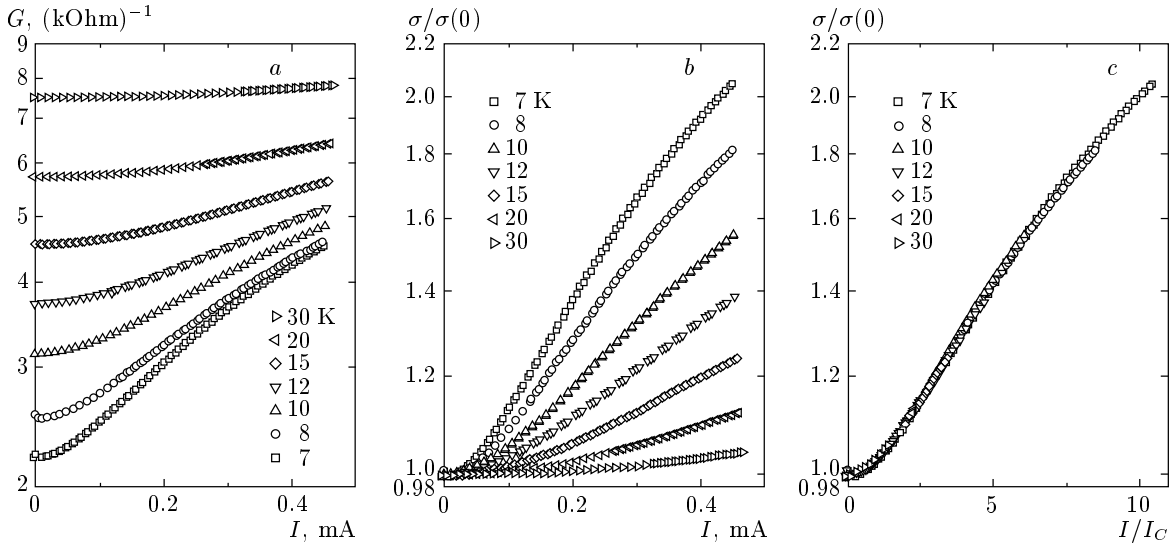

Fig. 9. *a*) Conductance as a function of the current through the $Gd_{0.14}Si_{0.86}$ sample № 3 at different temperatures. *b*) The same dependence when the conductivity is rescaled by the zero-current value $\sigma(0)$. *c*) The same dependence when the current is rescaled by the critical value I_C, to put in evidence the data collapse

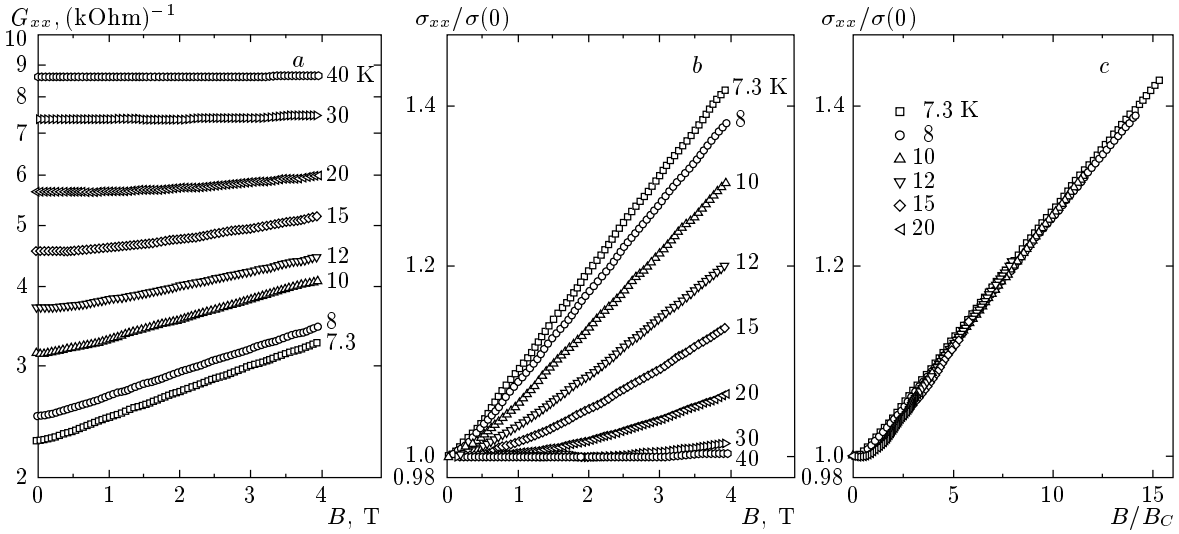

Fig. 10. *a*) Conductance vs magnetic field dependence for the $Gd_{0.14}Si_{0.86}$ sample № 3 at different temperatures. *b*) The same dependence when the conductivity is rescaled by the zero-field value $\sigma(0)$. *c*) The same dependence when the field is rescaled by the critical value B_C, to put in evidence the data collapse

are necessary to reveal details of the electron and magnetic structure of the drops.

In our theoretical model, we have neglected the low-temperature effects leading to the metal–insulator transition and associated with the Mott–Hubbard [6, 7] or percolation [13] mechanisms. Nevertheless, our experimental results are in accordance with the conclusions in Ref. [13] about the percolation character of the electron transport and the metal–insulator transition in the studied system.

We are grateful to Prof. F. Hellman and Dr. E. Helgren for sample preparation and critical remarks, to Prof. C. Di Castro, Prof. C. Castellani, and Prof. M. Grilli for valuable discussions. N. C. and V. T. were supported in part by the CRDF (grant RP2-2402-MO-02). V. T. was supported in part by the

invited-professor Program of the Center for Statistical Mechanics and Complexity (SMC) of the Istituto Nazionale per la Fisica della Materia (INFM), Unità di Ricerca (UdR) di Roma 1. S. C. was supported by the Italian MIUR, Cofin 2003, prot. 2003020239_006.

REFERENCES

1. F. Hellman, M. Q. Tran, A. E. Gebala, E. M. Wilcox, and R. C. Dynes, Phys. Rev. Lett. **77**, 4652 (1996).

2. W. Teizer, F. Hellman, and R. C. Dynes, Phys. Rev. Lett. **85**, 848 (2000).

3. F. Hellman, D. R. Queen, R. M. Potok, and B. L. Zink, Phys. Rev. Lett. **84**, 5411 (2000).

4. B. L. Zink, E. Janod, K. Allen, and F. Hellman, Phys. Rev. Lett. **83**, 2266 (1999).

5. B. L. Zink, V. Preisler, D. R. Queen, and F. Hellman, Phys. Rev. B **66**, 195208 (2002).

6. S. Kumar and P. Majumdar, Int. J. Mod. Phys. B **15**, 2683 (2001).

7. P. Majumdar and S. Kumar, Phys. Rev. Lett. **90**, 237202 (2003).

8. M. Sercheli, C. Rettori, and A. Zanatta, Brazilian J. Phys. **32**, 409 (2002).

9. I. M. Lifshitz, S. A. Gradescul, and L. A. Pastur, *Introduction to the Theory of Disordered Systems*, Nauka, Moscow (1982).

10. N. K. Chumakov, S. V. Gudenko, V. V. Tugushev, A. B. Davydov, V. I. Ozhogin, E. Helgren, and F. Hellman, J. Magn. Magn. Mater. **272–276**, 1351 (2004).

11. A. P. Levanyuk, V. V. Osipov, A. S. Sigov, and A. A. Sobyanin, Sov. Phys. JETP **49**, 176 (1979).

12. D. Haskel, J. W. Freeland, J. Cross, R. Winarski, M. Newville, and F. Hellman, Phys. Rev. B **67**, 115207 (2003).

13. L. Bokacheva, W. Teizer, F. Hellman, and R. C. Dynes, Phys. Rev. B **69**, 235111 (2004).